INNSPUB

International Journal of Biosciences | IJB |
ISSN: 2220-6655 (Print), 2222-5234 (Online)
http://www.innspub.net
Vol. 14, No. 2, p. 57-74, 2019

RESEARCH PAPER OPEN ACCESS

Biomechanical and histological assessment of titanium dental implants coated with strontium substituted hydroxyapatite and fluorapatite mixture

Hayder S. Hasan[1], Bayan S. Khalaf[2], Ban A. Jamil[3]

[1]*College of Dentistry, University of Baghdad, Baghdad, Iraq*

[2]*College of Dentistry, University of Baghdad, Baghdad, Iraq*

[3]*College of Dentistry, University of Baghdad, Baghdad, Iraq*

Key words: Dental implant coating, strontium substituted hydroxyapatite, fluorapatite.

http://dx.doi.org/10.12692/ijb/14.2.57-74 Article published on February 12, 20199

Abstract

Dental implants are considered a unique treatment alternative for the replacement of missing dentition. There is a strive for materials which increase bone formation in bone implant interface and improve osseointegration to offer immediate loading directly after placement with decreased time. The aim of the study was to assess the effect of nano strontium substituted hydroxyapatite and nano fluorapatite mixture coating of screw shaped commercially pure titanium at the bone implant interface by torque removal test and histological assessment in rabbit tibia. Commercially pure titanium was used to prepare 80 screws that were divided into machined surfaces (CpTi), coated with (SrHA), coated with (FA) and coated with mixture 50%SrHA + 50%FA (mixed). The dip coating process was used for producing a homogenous coating layer. Biomechanical and histological assessments were completed after 2 and 6 weeks of implantation. The results revealed that the mean removal torque value for the mixed group were significantly greater when compared with CpTi group, SrHA group, and FA group after 2 and 6 weeks There was more new bone formation around the screws for the mixed group for both healing intervals. Mixing nano strontium substituted hydroxyapatite and nano fluorapatite was more effective in increasing torque mean values, in addition to higher bone formation after 2 and 6 weeks as a result of combined effect of strontium, fluoride in coating.

* **Corresponding Author:** Hayder S. Hasan ✉ hayder.sabeeh@yahoo.com

Introduction

Osseointegrated dental implants are an ever more viable and successful treatment option for restoring edentulous spaces, demonstrating success rates of up to 96.8% (5, 6 and 10-16years respectively) (Jung *et al.,* 2008; Simonis *et al.,* ; 2010; Charyeva *et al.,* 2012).

The surface modification of dental implants, particularly their chemical and topographical structures, is an effective approach for obtaining dental implants with improved bioactivity (Zhang *et al.,* 2013). A nano-topographic surface can not only stimulate the proliferation, adhesion and osteogenic differentiation capability of osteoblast cells but also improve the osteoinductive potential for bone implants (Mendonça *et al.,* 2008; Li *et al.,* 2012).

Strontium, a trace element in the body of humans, has gained much concern because of its paired effect of stimulating bone formation and decreasing bone resorption (Buehler *et al.,* 2001). One of the strontium compounds, strontium ranelate, has been clinically used as an effective anti-osteoporotic oral drug for the prevention of fractures associated with osteoporosis by improving the quality of bone (Cianferotti *et al.,* 2013).

Strontium-substituted hydroxyapatite has been demonstrated to promote the osteoblast response and stimulate new bone formation more readily than pure hydroxyapatite (Xue *et al* 2007; Capuccini *et al.,* 2008; O'Sullivan *et al.,* 2010). Strontium-substituted hydroxyapatite inhibited bone resorption and improved bone formation (Marie *et al.,* 1993; Grynpas MD *et al.,* 1996; Ammann *et al.,* 2004). In addition, it had positive effects in increasing the number of osteoblasts and reducing the number and activity of osteoclasts (Canalis *et al.,* 1996; Chang *et al.,* 1999).

Peri-implantitis remains the major burden to the long-term usage of dental implants. With increasing concern of antibiotic resistance, there was considerable attention in the preparation of antimicrobial coatings that also improved osseointegration[17]. Fluorapatite was one such potential coating material. Alhilou and his co-workers in 2016 (Alhilou *et al.,* 2016) founded that fluorapatite may be used as a coating for dental implants that shows significant antibacterial activity against bacteria associated with peri-implantitis. Also, fluorapatite has been shown to improve the bone apposition rate in early osteogenesis (Dhert *et al.,* 1993). In addition, fluorapatite has the ability for releasing fluoride ions, which have an osteoinductive effect on bone (Ohno *et al.,* 2013). The aim of this study was to assess the effect of coating commercially pure titanium implants with nano strontium substituted hydroxyapatite and nano fluorapatite mixture at the bone implant interface by torque removal test and histological assessment in rabbit tibia.

Materials and methods

Substrate Preparation

Grade II commercially pure titanium rods were used for preparing 11 circular discs of 20 mm diameter and 2 mm thickness. The discs were grinded by using silicon carbide paper at 500 grit to bring it to an even smooth surface using a rotated grinding motion at 250 rotations per minute (rpm) for 2 minutes with a final thickness of 1.99 mm. 80 screws were prepared with a length of 8 mm and diameter of 3 mm. The smooth part was 3 mm in length and the threaded part was 5 mm with a distance of 0.6 mm between each thread. The head of the implant had a slit of 1 mm width and 1.5 mm depth to fit the screwdriver and torque meter during insertion and removal process.

Ultrasonic cleaning with ethanol absolute (≥ 99.8%) for 15 minutes was used to remove the debris and contaminants from the screws. Finally, they were washed with distilled water and dried at room temperature (Refaat and Hamad 2016).

Coating of the substrates & sterilization

The first suspension was prepared by dissolution of 0.01 g of phosphorus pentoxide (p205) in 50 ml of

ethanol and heated for 30 minutes at 45°C on a hot stirrer. Then 7 g of nano strontium substituted hydroxyapatite powder was added to the solution. The temperature was kept at about 45°C then the mixture was left for half an hour over a stirrer to gain homogenous solution. The suspension preparation was the same for the other two suspensions with exception of addition of the test material.

The second suspension included 7g of fluorapatite in fluorapatite suspension and the third suspension included 3.5 g of strontium substituted hydroxyapatite with 3.5 g of fluorapatite in mixed suspension (Al-Molla *et al.,* 2014).

Sample grouping

Eleven discs were divided into the following groups:
Three discs for thickness measurement analysis.
Four discs for XRD.
Four discs for SEM and EDX.
Eighty screws were divided into the following groups:
Twenty screws with machined surfaced commercially pure titanium (CpTi).
Twenty screws coated with strontium substituted hydroxyapatite (SrHA).
Twenty screws coated with fluorapatite (FA).
Twenty screws coated with strontium substituted hydroxyapatite (SrHA) and fluorapatite (FA) mixture at percentage 1:1 (mixed).

The prepared discs were immersed into the dipping solution for 30 seconds and then removed and left to dry for one minute at room temperature. The dip coating process was performed electronically using a special dip-coating apparatus at speed of 10 cm/min. This process was repeated to increase the coating thickness. Then the coated screws were sintered at 700 °C for 30 min. for densification using a carbolite furnace. The treatment was done under inert gas (argon) to preclude oxidation of the samples. The same procedure was used for coating the implant screws (Bhaskar 1991; Li *et al.,* 2010).

The coated screws were sterilized by gamma radiation and kept in a single self-sealing sterilization pouch till the day of surgery.

Characterization of the coatings

Phase analysis was employed on commercially pure titanium discs and coatings by using an X-ray phase machine (Shimadzu lab XRD – 6000, Japan). Scanning of the samples was perused with Cu Kα X-ray source in the 2θ range from 10° to 80° with one degree. the peak indexing was carried out based on the JCPDS (joint committee on powder diffraction standards) international centre for diffraction data, ICDD File # 44-1294 for Ti # 09-0432) for HA, # 15-0876 for FA). The surface topography and morphology of coatings was measured by using Scanning Electron Microscope (SEM) (VEGA3 LM | TESCAN, Czech.). Energy-dispersive X-ray spectroscopy (EDX) was done for the coated samples within the SEM instrumentation. Microprocessor coating thickness gauge (Erichsen Mini test 3000. W-Germany) was used for measuring thickness of coated samples.

Surgical procedure

Twenty healthy New Zealand adult male white rabbits (Oryctolagus cuniculus) were used weighing 1.5 - 2 kg and about 11 months of age. They were left for 2 weeks in the same environments before surgical procedure. Subcutaneous single dose of ivermectin injection (10 mg) was given to insure that the animals were parasite free. On the day of surgery the rabbits were anesthetized then the legs were shaved, washed, and then decontaminated by iodine with 70% ethanol. The incision was done on the lateral side of rabbit's leg to expose the medial side of the tibia. The bone was penetrated with a round bur 1.8 mm in diameter to make 2 initial holes with 1 cm distance between them, with intermittent pressure and continuous irrigation with normal saline for cooling. The preparation site was enlarged gradually with a round bur to 2.8 mm. In the left tibia, CpTi screw was inserted in the first hole (proximal one) via a screwdriver until the screw was inserted completely into the bone and the mixed coated screw was inserted in the second hole (distal one). While in the right tibia, SrHA coated screw was inserted in first

hole (proximal one) and FA coated screw was inserted in the second hole (distal one). The screws were finally screwed in place with torque meter at nearly 10 N.cm. The muscles were sutured with 3/0 absorbable catgut suture and by skin suturing with 3/0 silk suture. Local antibiotic spray (oxytetracycline) was applied over the operation site and followed by injection with systemic antibiotic (oxytetracycline).

Biomechanical test

Sixteen rabbits were used for biomechanical testing and were divided equally into two groups; according to healing intervals of 2 and 6 weeks. The rabbits were anesthetized and an incision was made at the lateral side of the tibia to reflect the muscles and fascia to expose the implants. A torque removal test was carried out with a digital torque meter (professional torque meter, TQ 8800, Mrclab, China) by engaging the screw driver of the digital torque meter into the slit of the implant head to determine the peak torque required to unscrew the implant from its bed.

Histological test

Four rabbits were divided equally into two groups, according to healing intervals of 2 and 6 weeks. The rabbits were given an overdose of anesthetic solution and the bone-implant block was cut by a disc cutter with low rotating speed with cooling by normal saline. The cut was at a distance of about 0.5 cm away from the implant to make a bone-implant block for histological assessment. Blocks were directly kept in freshly prepared formalin of 10% for fixation for 3 days. The bone-implant blocks were decalcified by immersing them in 10% formic acid for 2-3 weeks and tested by penetration of a narrow needle to the depth of the bone-implant block [23]. After that, the bone block was cross sectioned along the length of the implant with a small scalpel into equally 2 parts.

The bone tissue was dehydrated through placing it in alcohol with serial concentrations (70%, 80%, 90% and absolute alcohol for 60 minutes for each concentration). Then, the bone samples were passed through two changes of xylene for 15-20 min. Each sample was placed in the center of melted paraffin dish and the dish was placed inside a constant-temperature oven regulated to 60 ^{o}C for 30min. Paraffin wax was used for immersing, so that paraffin replaced all of the xylene in the tissue (Linder 1985).

The prepared samples were sectioned with a microtome to obtain serial sections of 5 µm of thickness to place on a slide. 10 sections were made for each block of the test groups and for each time interval. The tissues were stained with haematoxylin and eosin stain for 10 minutes. An optical microscope (Olympus /542037, Japan) was used for histological examination.

Results

In this study the x-ray phase analysis of the samples for all the test groups showed narrowed peak widths with increased peak intensities indicating high degree of crystallinity, as seen in figures 1, 2, 3, and 4.

Table 1. Paired sample t-test comparison for torque removal test at 2 and 6 week intervals.

		t	df	Sig. (2-tailed)
Pair 1	CpTi 2 weeks - CpTi 6 weeks	-2.199	7	.064
Pair 2	Mixed 2 weeks - mixed 6 weeks	-10.119	7	.000
Pair 3	SrHA 2 weeks - SrHA6 weeks	-2.278	7	.057
Pair 4	FA 2 weeks – FA 6 weeks	-6.619	7	.000

Table 2. Descriptive statistical analysis for torque removal test after 2 week interval.

Groups	N	Mean	Std. Deviation	Std. Error	95% Confidence Interval for Mean		Minimum	Maximum
					Lower Bound	Upper Bound		
CpTi	8	11.25	2.252	.796	9.37	13.13	8	14
mixed	8	16.25	2.188	.773	14.42	18.08	13	19
SrHA	8	11.88	2.532	.895	9.76	13.99	9	15
FA	8	12.88	2.800	.990	10.53	15.22	10	17

It was evident that the CpTi and FA samples (fig. 1, 3) show a perfect matching to ICDD file # 44.1294 for titanium, # 15-0876 for FA, respectively. Meanwhile for the SrHA and mixed groups the samples showed a good match with hydroxyapatite standard (ICCD file # 09-0432 for HA) except some peeks with minor shifts towards smaller 2θ values.

Table 3. ANOVA table for torque removal test after 2 week interval.

	Sum of Squares	df	Mean Square	F	Sig.
Between Groups	119.125	3	39.708	6,589	.002
Within Groups	168.750	28	6.027		
Total	287.875	31			

Table 4. Multiple comparison test (Tukey HSD) for torque removal test after 2 week interval.

Dependent Variable		Mean Difference (I-J)	Sig.
CpTi	mixed	-5.000*	.002
	SrHA	-.625	.956
	FA	-1.625	.556
mixed	SrHA	4.375*	.007
	FA	3.375*	.048
SrHA	FA	-1.000	.847

Table 5. Descriptive statistics for torque removal test after 6 week interval.

Groups	N	Mean	Std. Deviation	Std. Error	95% Confidence Interval for Mean		Minimum	Maximum
					Lower Bound	Upper Bound		
CpTi	8	14.63	3.292	1.164	11.87	17.38	10	18
mixed	8	22.13	2.232	.789	20.26	23.99	20	26
SrHA	8	16.63	4.779	1.690	12.63	20.62	11	26
FA	8	19.38	1.768	.625	17.90	20.85	17	23

SEM micrographs of the surface morphology of the CpTi, SrHA, FA and mixed coated samples are represented in (Figures 5, 6, 7&8). The surface morphologies SEM micrographs for the CpTi samples showed parallel grooves which were caused by machining and polishing without topographical features (Figure 5). Micrographs of SrHA, FA, and mixed samples (Fig. 6, 7& 8) showed that the coatings were uniform, dense, and microporous with agglomerated particles. Both micrographs of the samples for the SrHA and mixed groups showed micro cracking but mixed samples had less micro cracking. Meanwhile, the micrograph for the FA group was free cracking.

Table 6. ANOVA table for torque removal test for 6 week interval.

	Sum of Squares	df	Mean Square	F	Sig.
Between Groups	256.375	3	85.458	8,181	.000
Within Groups	292.500	28	10.446		
Total	548.875	31			

Table 7. Multiple comparison test (Tukey HSD) for torque removal test for 6 week interval.

Dependent Variable		Mean Difference (I-J)	Sig.
CpTi	mixed	-7.500*	.000
	SrHA	-2.000	.609
	FA	-4.750*	.031
mixed	SrHA	5.500*	.010
	FA	2.750	.342
SrHA	FA	-2.750	.342

Elemental mapping and chemical composition (EDX) of the samples for all of the groups are represented in figures 9, 10, 11 & 12.

The EDX analysis of the CpTi sample (Fig. 9) showed that it was made up of 100% titanium. SrHA dip coated sample (Fig. 10) showed the presences of 3% strontium and FA dip coated sample (Fig. 11) showed that 3.5% fluoride was present. While, the mixed dip coated sample (Fig. 12) showed that both 2.1% strontium and 1.4% fluoride were found in the coating.

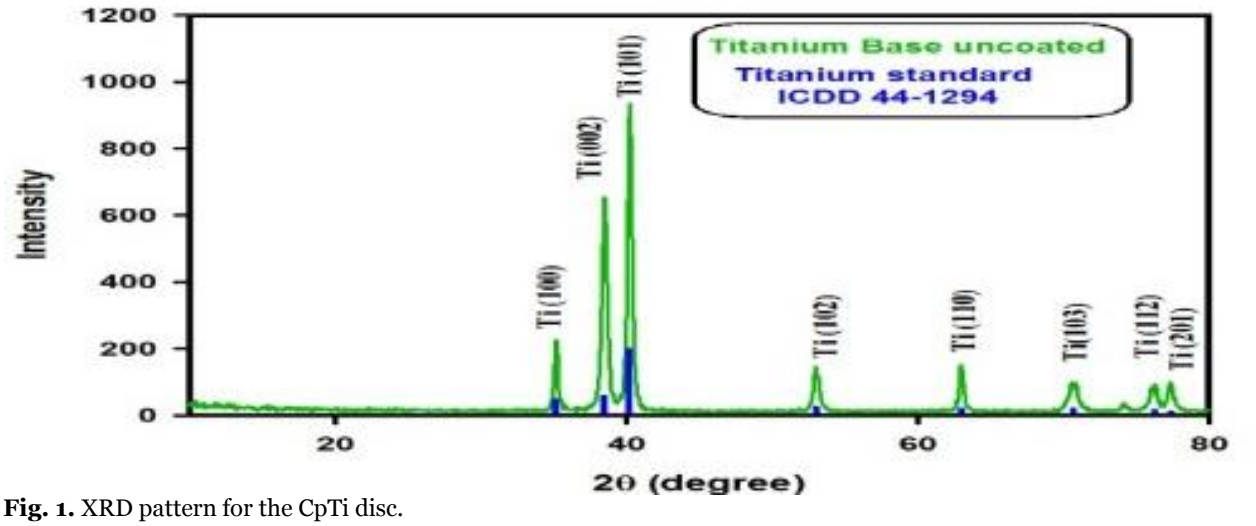

Fig. 1. XRD pattern for the CpTi disc.

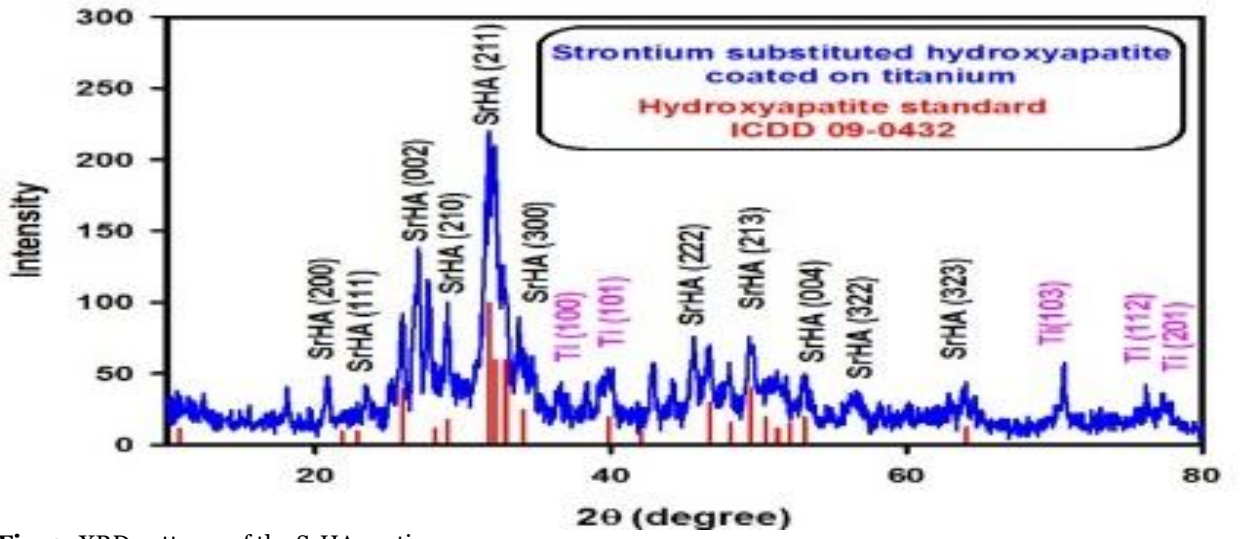

Fig. 2. XRD patterns of the SrHA coating.

The thickness of the coating layer of all dip coated samples was different with the SrHA group showing the thinnest layer and the mixed group with the thickest coating (Fig. 13).

Biomechanical test

In this study, the removal torque test was used for evaluating the interface mechanics. The results of the paired sample t-test revealed a highly significant difference at $P \leq 0.01$ in the mixed and the FA groups, as seen in table 1. The torque mean value of the mixed group was the highest for both 2 and 6 weeks intervals when compared with other groups (table 2 and 5).

The ANOVA test showed a highly significant difference among the experimental groups for 2 and 6 weeks of healing intervals (table 3 and 6). Multiple comparison test (Tukey HSD) for 2 weeks healing interval showed that there was highly significant

difference between the CpTi group and the mixed group and between the mixed group and the SrHA group, while it was significantly different between the mixed group and FA group. The results for the 6 weeks healing interval showed a highly significant difference between the CpTi group and the mixed group and significant difference between the CpTi and FA groups. Also, there was a highly significant difference between the mixed and SrHA groups (table 4and 7).

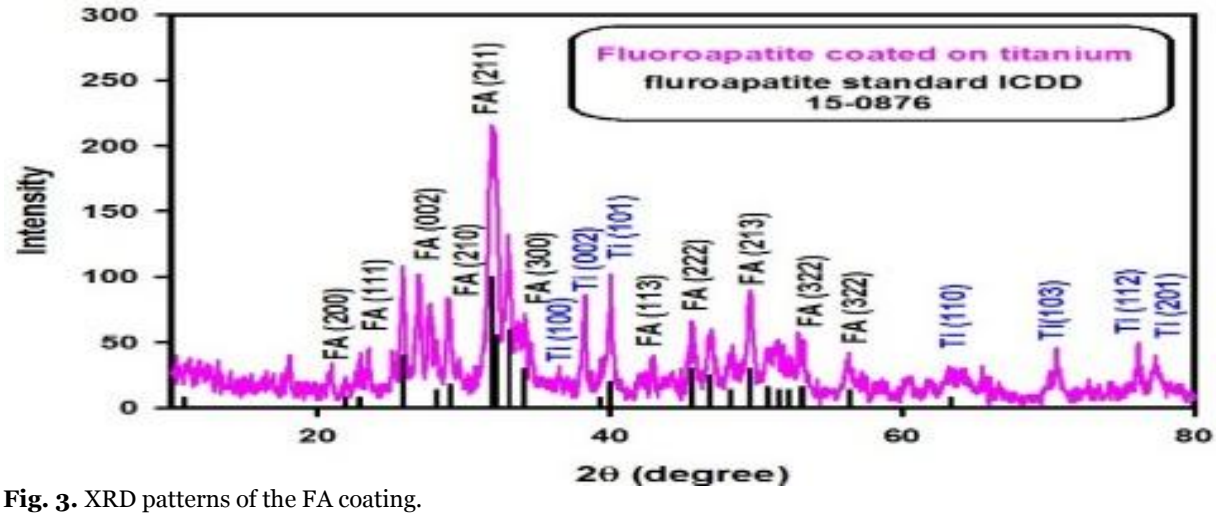

Fig. 3. XRD patterns of the FA coating.

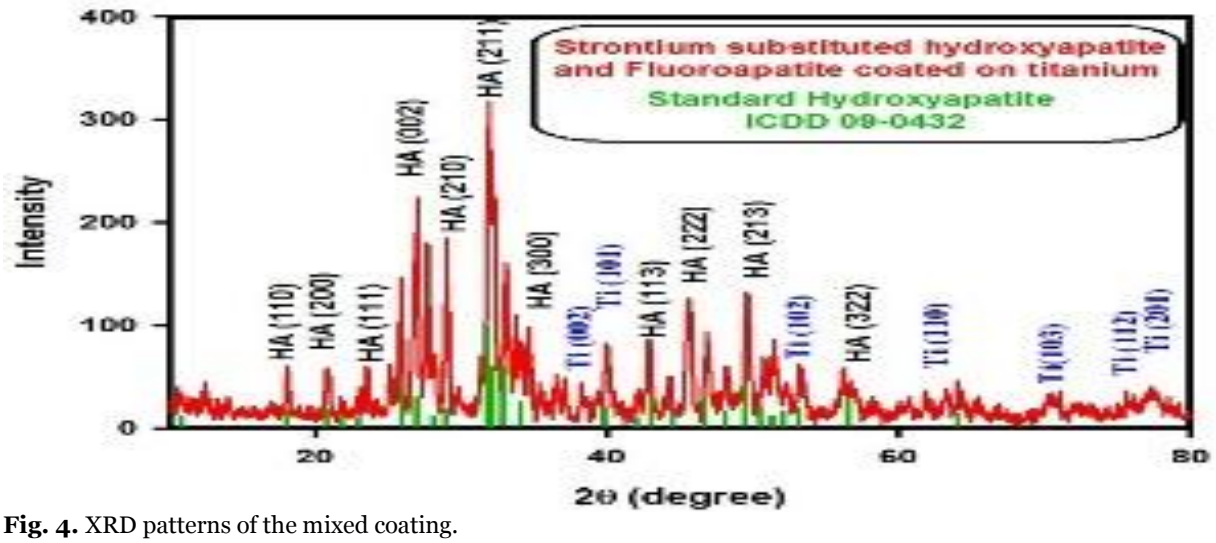

Fig. 4. XRD patterns of the mixed coating.

Histological findings

The implant surface structure played an important role in the Osseointegration which, in turn, affected the Biological responses through the alterations in composition and structure of the bone-implant interface at different healing intervals (Azzawi *et al.,* 2018).

Histological features after 2 weeks of implantation

Microphotograph view of implant site of 2 weeks interval of control group showed new bone deposition by osteoblasts at apex of thread regions, fibroreticular tissue with fibroblasts, as illustrated (fig14). Bone deposition at apical areas of thread regions was detected in the histological examination of the SrHA group and was surrounded by marrow tissue (fig15).

The view of bone-implant section of the FA group showed the newly deposited bone enclosing numerous osteocytes and rimmed by formative osteoblasts (fig16). Histological examination of mixed coated group showed operative site where bone

trabeculae rimmed by osteoblasts and osteocytes embedded in bone is shown (fig 17).

Histological features after 6 weeks of implantation

Histological microphotograph of the CpTi group of the 6 weeks interval showed mature dense bone with osteocytes that appeared regularly arranged around Haversian system (fig18).

The view of the SrHA group showed a thread of dense mature bone enclosing osteocytes also osteoblasts were detected (fig19).

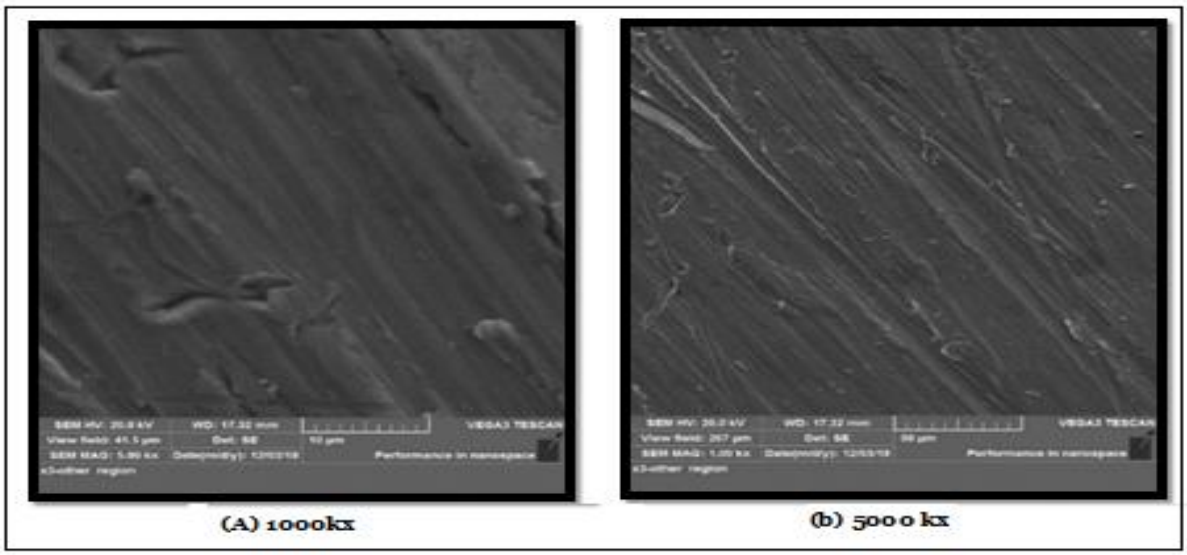

Fig. 5. SEM micrographs of surface morphology of CpTi disc.

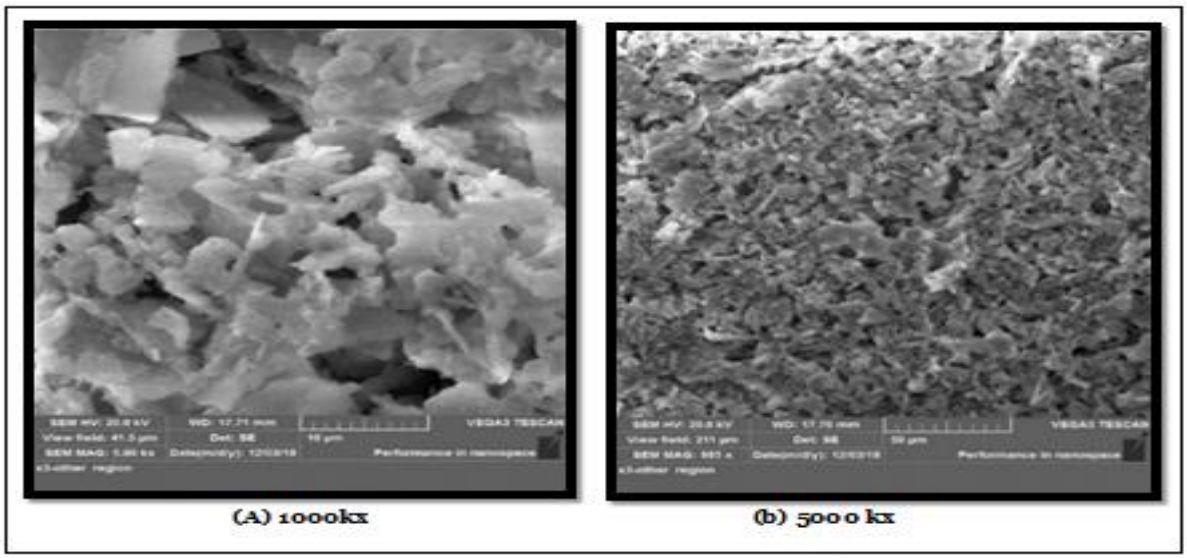

Fig. 6. SEM micrographs of surface morphology of SrHA Coating.

Meanwhile, FA group showed mature bone at thread areas with enclosing marrow tissue with osteoblasts seen at peripheries (fig 20). As illustrated in magnified histological view of mixed coated group of 6 weeks interval that mature bone filled the thread regions and reversal lines separating between old and new bone (fig21).

Discussion

X-ray phase analysis of the coated samples showed that the presence of strontium and fluoride in the coating layer was not affected and with structure of hydroxyapatite. Nevertheless, presences of a small shifts in some peeks (Fig. 2 and 4) for the SrHA and mixed samples towards smaller 2θ values happened

due to substitution of the large strontium atom with the smaller calcium atom in hydroxyapatite lattice.

Surface Morphology

The surface morphologies (SEM) for all coated samples showed microporous features and this may have been due to ethanol evaporation during coating process or result from coalescence of particles in all coated samples as aggregates led to the formation of porous agglomerates. This microporosity made the surface of the coating material rougher which has a positive effect on osseointegration and bone formation.

These findings agree with studies of Kavitha (Kavitha *et al.*, 2015) and Raucci (Raucci *et al.*, 2015).

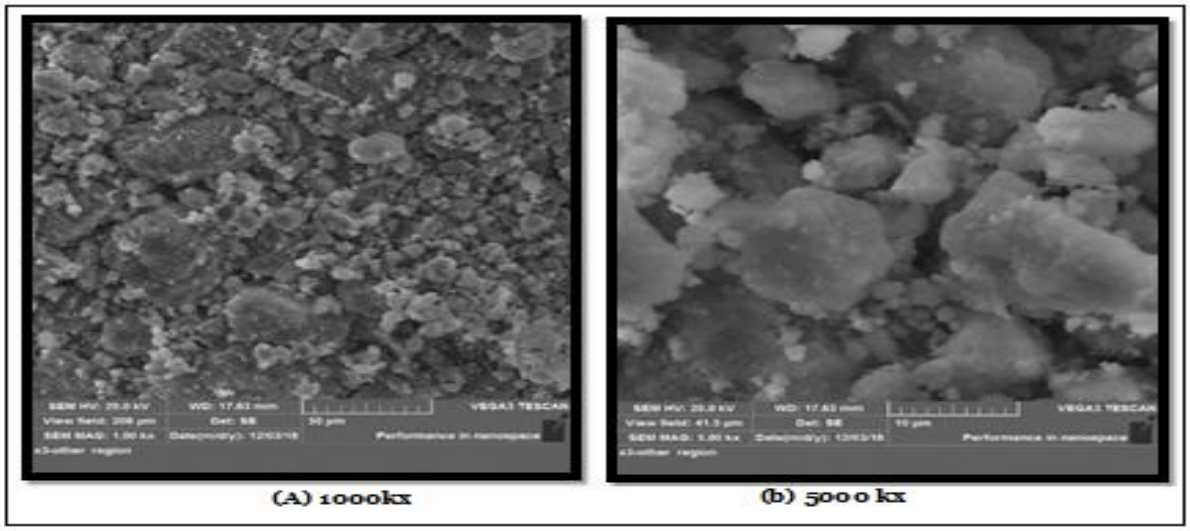

Fig. 7. SEM micrographs of surface morphology of FA coating.

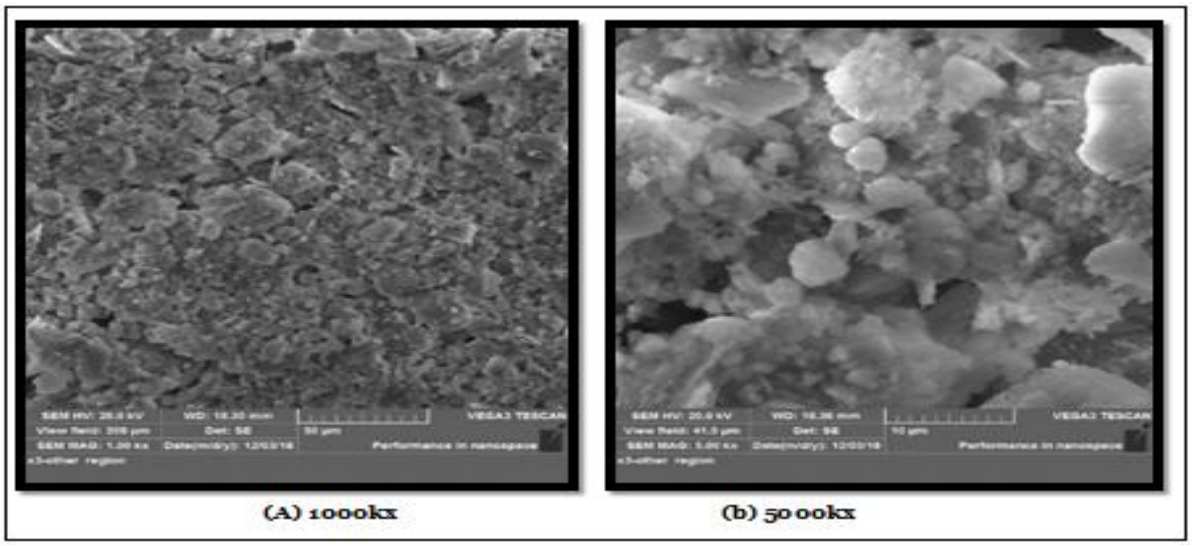

Fig. 8. SEM micrographs of surface morphology of mixed coating.

The micro cracking (Fig. 6 and 8) in the coating layer of the samples for the SrHA and mixed groups was probably due to the shrinkage that occurred during the thermal processing. Absence of cracks in FA group could suggest that there was no shrinkage in the coating (Fig. 7).

EDX

EDX results of all coated samples confirmed the presence of homogeneous distribution of strontium, fluoride, calcium, phosphate, oxygen in coatings. This indicated that coating material was successfully precipitated on the surface of the substrate.

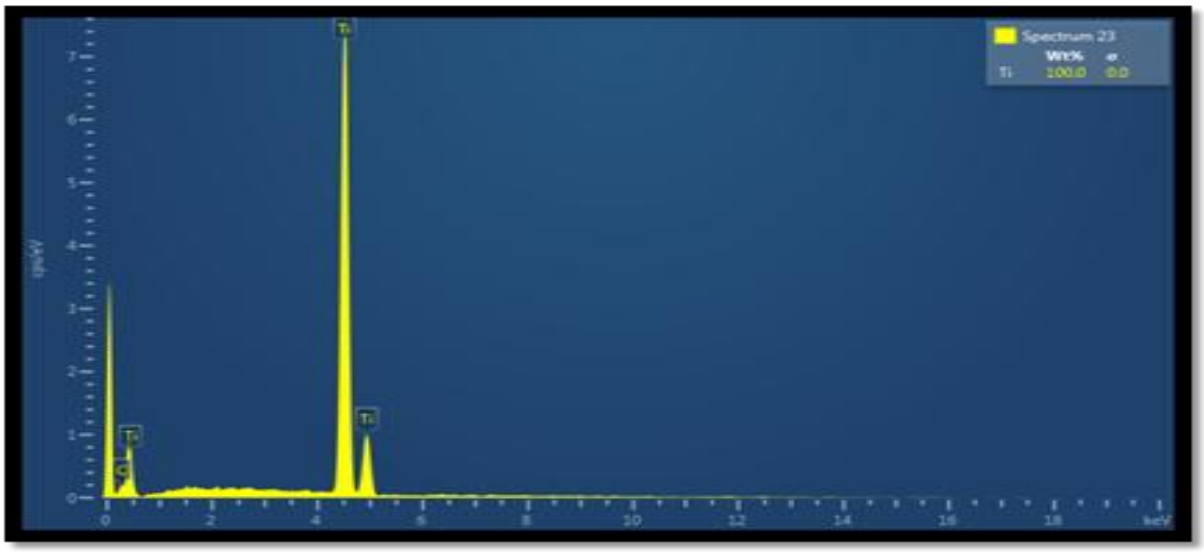

Fig. 9. EDX analysis for CpTi.

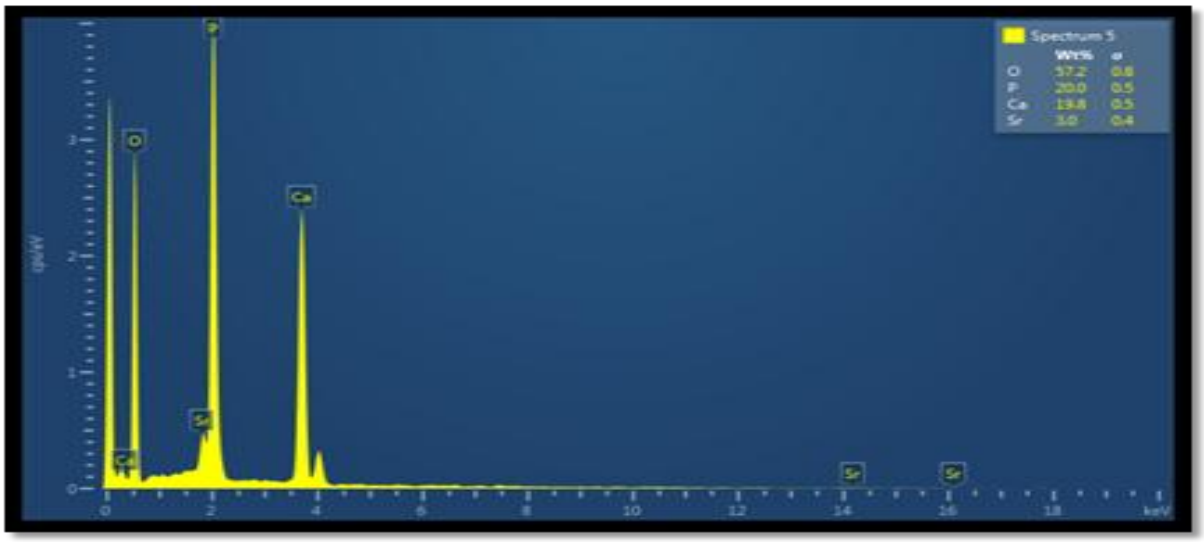

Fig. 10. EDX analysis for SrHA coating.

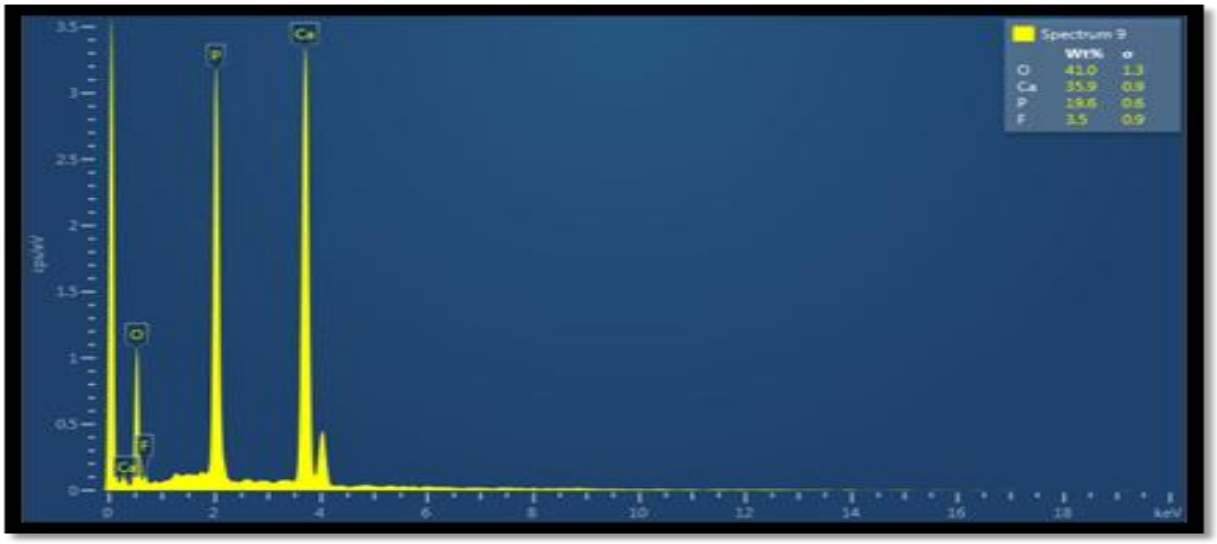

Fig. 11. EDX analysis for FA Coating.

Histological Analysis

The removal torque test was used mainly for probing for the interface mechanics and represented a sign of the presence of osseointegration.

Many studies used the removal torque test because it was considered a vital parameter for studying and comparing osseointegration of screw shaped implants (Kim *et al.,* 2016; Park*et al.,* 2016; Hamad *et al.,* 2018; Hassan *et al.,* 2018). Also, histological analysis could be considered one of the reliable methods to evaluate osseointegration of implants that could be achieved at any time of implantation (Alsumi *et al.,* 2007).

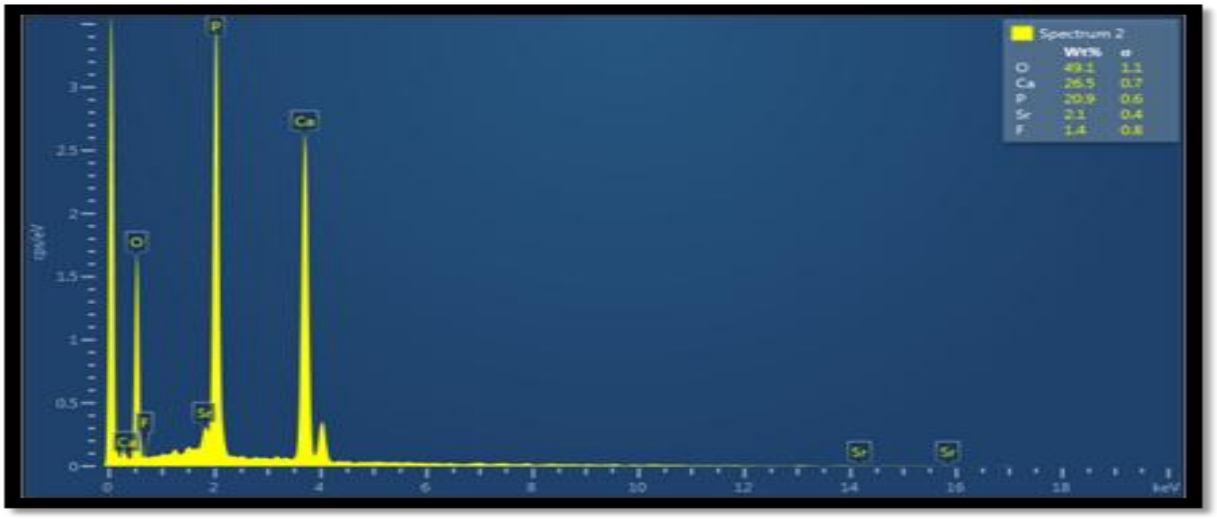

Fig. 12. EDX analysis for mixed Coating.

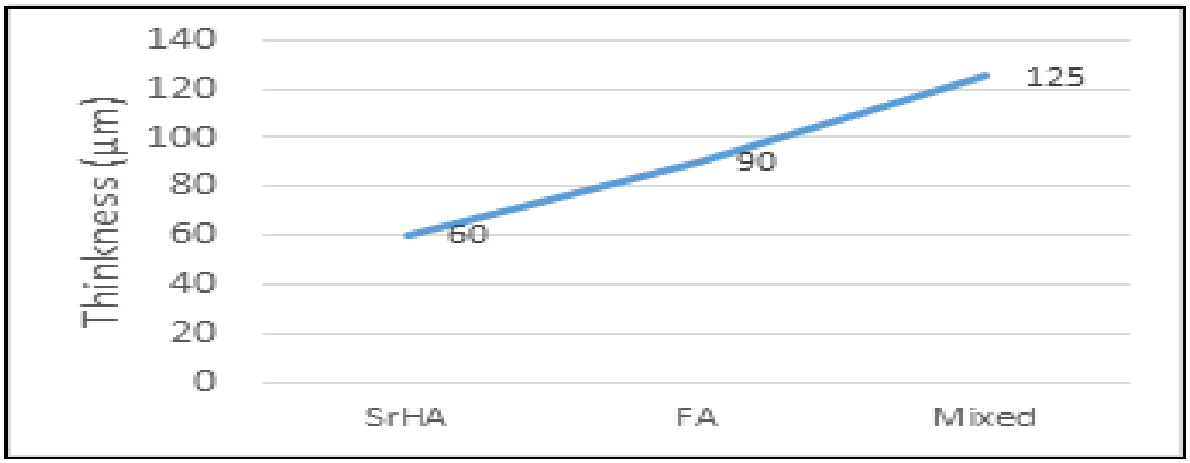

Fig. 13. Coating thickness for all the coatings.

The results of this study revealed that the removal torque values increased with time for all groups as a result of bone formation and remodeling around the implants during the healing interval with improved osseointegration. This indicated that the coating materials were not toxic, well tolerated by biological tissues of study models, and had a positive influence on bone tissues by stimulating bone formation. This finding agreed with that of Refaat and Hamad (Refaat and Hamad 2016). Al-Khafaji (Al-Khafaji 2015) stated that osseointegration could be achieved when coated implants were implanted in living bone tissue with a good biological environment for bone formation. Those findings were confirmed by the results of this study and confirmed by the histological analysis where bone deposition and maturation was noticed in all groups. After 2 weeks of implantation, histological examination of coated groups showed more obvious

new bone trabecular deposition rimmed by osteoblast and enclosing numerous osteocytes at the thread region as compared to uncoated CpTi implants (control group). After 6 weeks of implantation, histological features for all groups showed mature dense bone with osteocytes regularly arranged around harversian system.

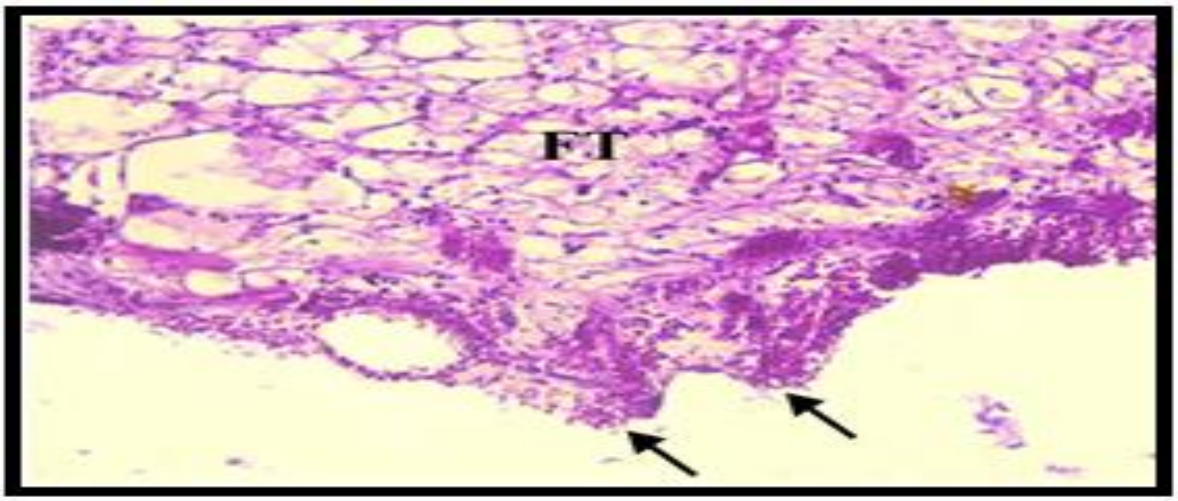

Fig. 14. Histological view of CpTi screw site after 2weeks shows thread region (arrows) fibroreticular tissue (FT), H&E stain 20x.

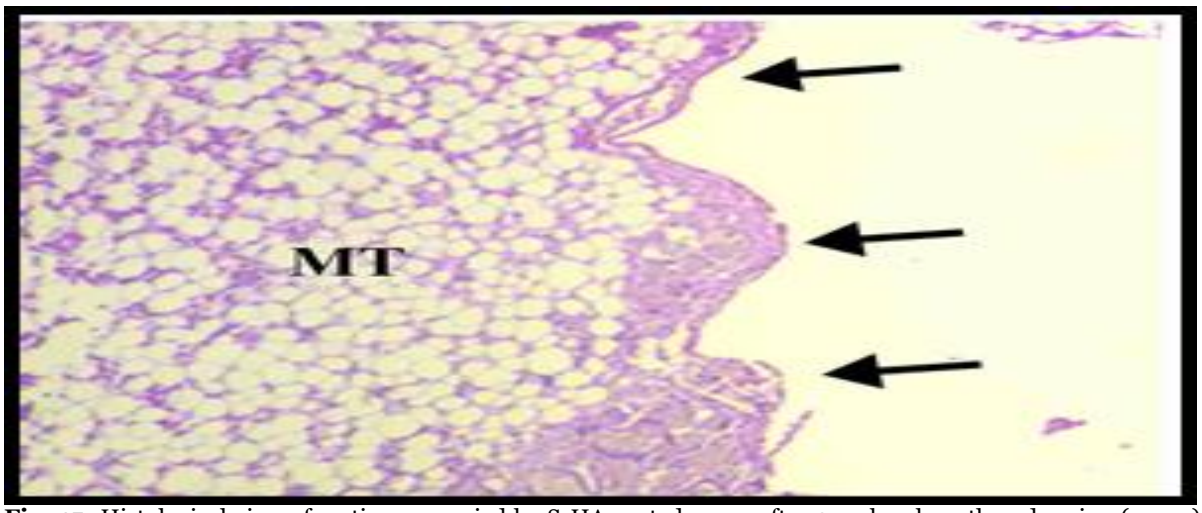

Fig. 15. Histological view of sections occupied by SrHA coated screw after 2week show thread region (arrow), where new bone was deposited at apex of threads and marrow tissue (MT), H&E stain 10x.

Effect of Strontium Hydroxyapatite

After 2 and 6 weeks of implantation the SrHA group recorded higher mean values compared with the CpTi group. This was due to positive effects of strontium in hydroxyapatite for exciting osteoblast formation and blocking osteoclast triggering and thus decreasing resorption. The mechanism of action of strontium is based on ion release and strontium becomes absorbed by ion exchange processes with calcium or binds to osteoid proteins, or the integration of strontium ions into the hydroxyapatite crystal of the bone tissues (Jani and AL-Ameer 2016). Another explanation is that strontium replaces calcium in osteoblast-mediated processes and enhances osteogenesis via osteoblast formation while preventing osteoclastic resorption. In addition, strontium was known to enhance the differentiation of osteoblasts into osteocytes (Atkins *et al.,* 2009). Influence of strontium is based on the calcium sensing receptor (CaSR) interaction that improves osteoblast

proliferation (Bonnelye *et al.,* 2008), inhibits pre-osteoclast maturation, and induces apoptosis in mature osteoclasts (Chattopadhyay *et al.,* 2007; . Hurtel-Lemaire *et al* 2009).

Effect of FA on Bone Formation

After 2 and 6 weeks of implantation FA group recorded higher mean values when compared with the CpTi. These results may be explained by the effect of FA on bone formation. FA has the ability to release fluoride ions which may be incorporated in bone lattice. Due to its affinity for calcium, fluoride tends to accumulate in bone and replace the hydroxyl ions with hydroxyapatite crystals making it more stable and more bioactive (Whitford *et al.,* 1999).

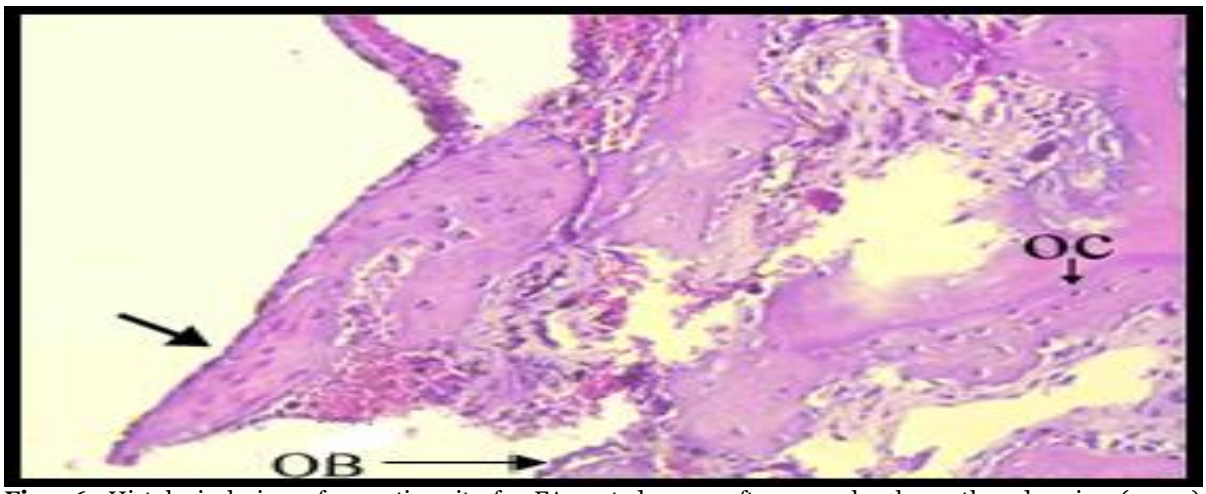

Fig. 16. Histological view of operative site for FA coated screw after 2 weeks shows thread region (arrow), osteocytes (OC), osteoblasts (OB) H&E 20x.

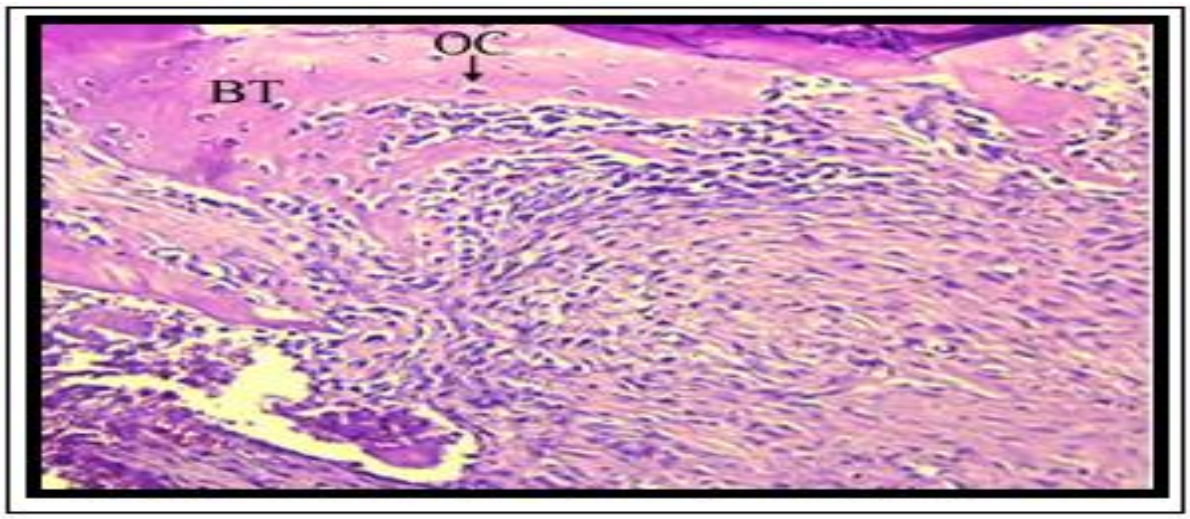

Fig. 17. Histological view of mixed coated screw site shows newly formed bone trabeculae (BT), osteocytes (OC) distributed inside the bone H&E 20x.

The presence of fluoride may contribute to altered equilibrium of the apatite resulting in distinct ionic balance in the perimaterial microenvironment which may increase bone formation (Qiao *et al.,* 2018). In addition to the osteoinductive property, the antibacterial action of FA elucidated either by indirect mechanisms by affecting on metabolism and growth of oral bacteria. The fluoride has weak-acid character that alters the permeability of the membrane to protons and compromises F-ATPase molecules, which would usually regulate a proton gradient (Marquis 1995; Marsh and Martin 1999).

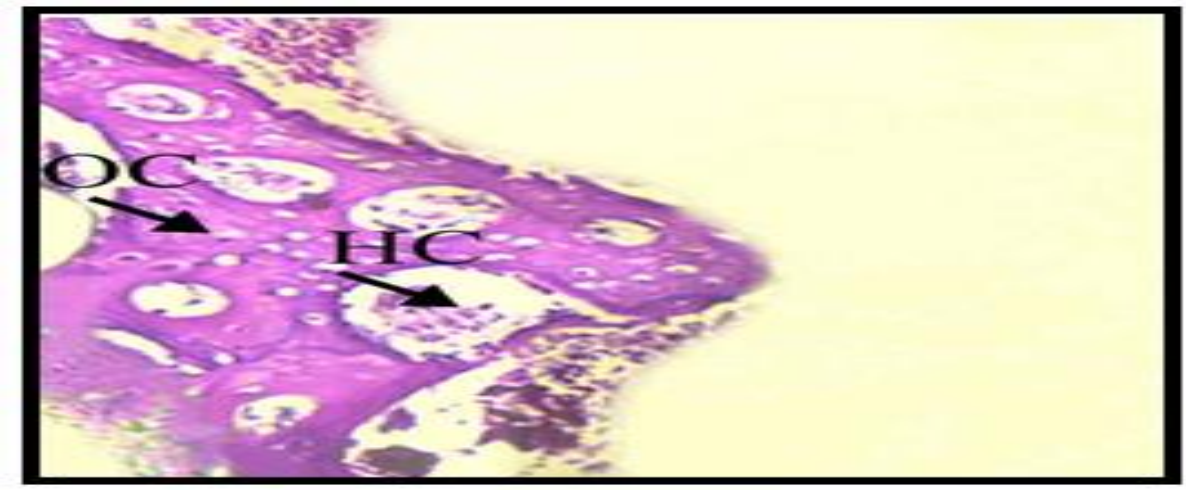

Fig. 18. Histologic view of section occupied by CpTi implant after 6 weeks shows thread area occupied by haversian canals (HC), surrounded by osteocyte (OC) H&E stain 20x.

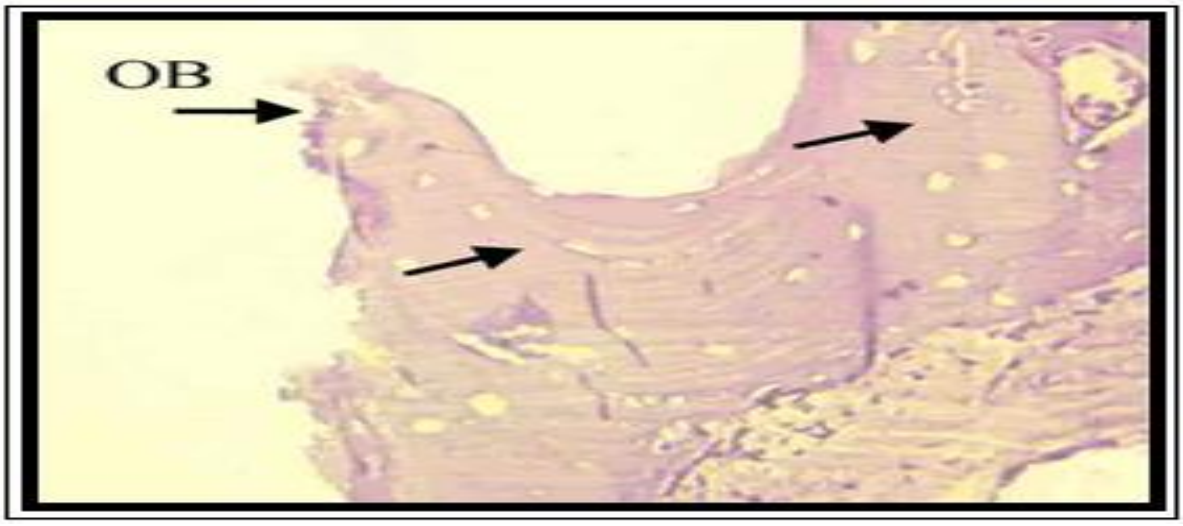

Fig. 19. Histological view of operative site for SrHA coated screw after 6 weeks shows thread region with mature dense bone (arrow), osteoblasts (OB) H&E 40x.

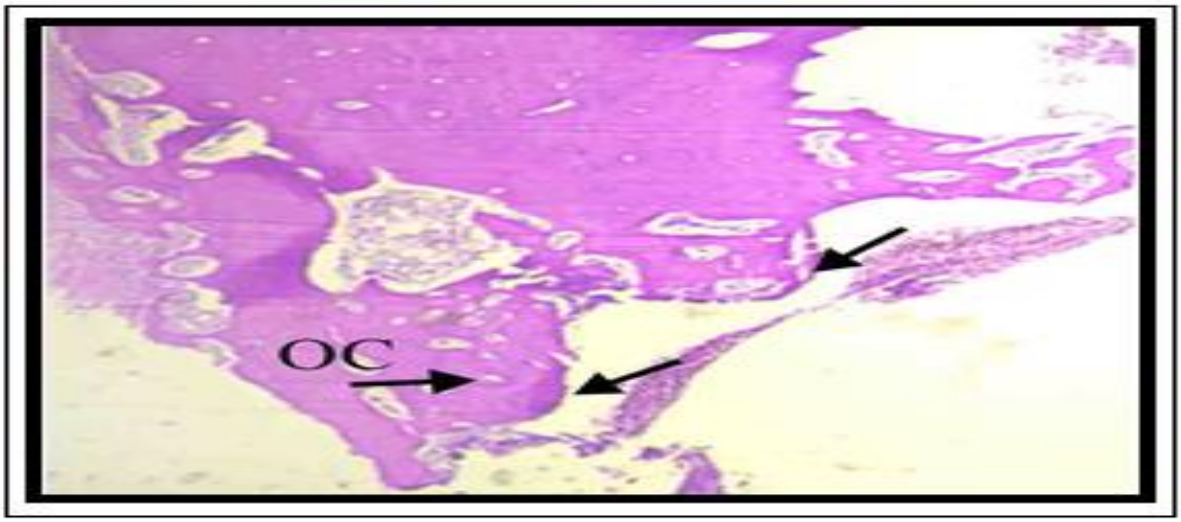

Fig. 20. Histological view of operative site for FA coated screw after 6weeks show thread region (arrows) of dense mature bone, osteocyte (OC) H&E stain 20x.

Or by direct antimicrobial action by binding and inhibiting a number of metabolic enzymes (Vogel *et al.,* 2002; Takahashi and Washio 2011). The Mixed coated screws had significantly increased removal torque mean values which were 16.25 N.cm and 22.13 N.cm for both healing intervals respectively when compared with all of the other groups. This indicated the presence of strong bond strength at interface between the bone and implant which may have resulted from the combined effect of fluoride and strontium ions in the hydroxyapatite coating on bonetissues.

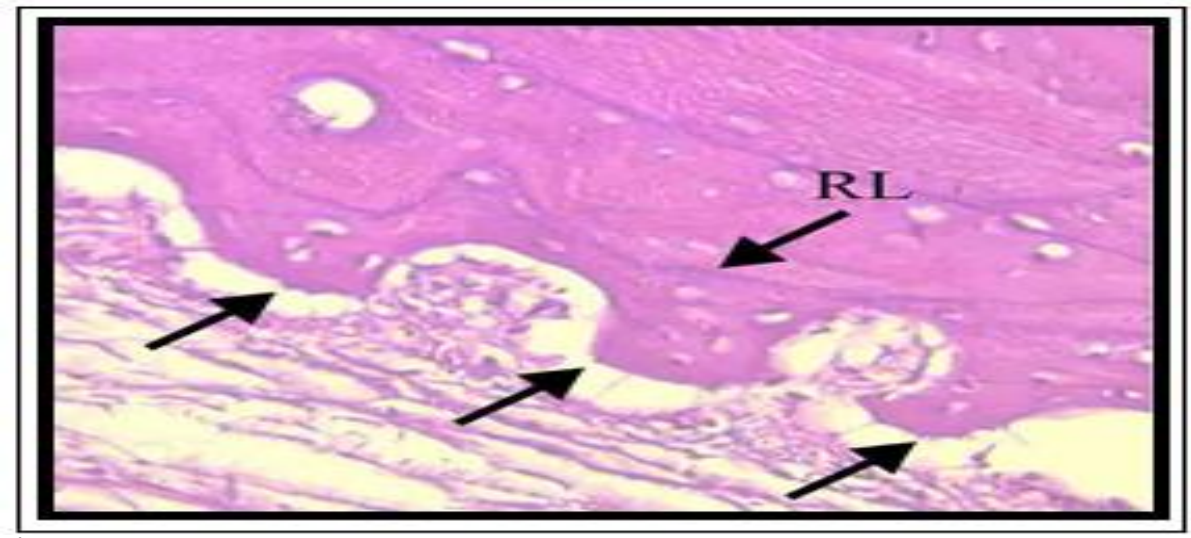

Fig. 21. Histological view of section occupied by mixed coated implant after 6 weeks of implantation shows many threads of mature bone, reversal line (RL)is seen also H&E stain 40x.

The result of this study indicated that mixing SrHA and FA was more effective in increasing torque mean values for 2 and 6 weeks intervals due to combined effect of strontium and fluoride in coating on bone formation and osseointegration.

Conflict of Interest

The authors and planners have disclosed no potential conflicts of interest, financial or otherwise.

References

Alhilou A, Do T, Mizban L, Clarkson BH, Wood DJ, Katsikogianni MG. 2016. Physicochemical and antibacterial characterization of a novel fluorapatite coating. ACS OMEGA **1(2),** 264-276.

Al-khafaji RN. 2015. Osseointegration assessment of Al2O3-AgNO3 Mixture on Cp Ti implants (In vivo study), Master thesis, College Of Dentistry, University of Baghdad.

Al-Molla BH, Al-Ghaban N, Taher A. 2014. Immunohistochemical evaluation: The effects of propolis on osseointegration of dental implants in rabbit's tibia. Journal of Dental Research and Review, **1(3),** 123-131.

Ammann P, Shen V, Robin B, Mauras Y, Bonjour JP, Rizzoli R. 2004. Strontium ranelate improves bone resistance by increasing bone mass and improving architecture in intact female rats, Journal of bone and mineral research **19(12),** 2012-2020.

Atkins GJ, Welldon KJ, Halbout P, Findlay DM. 2009. Strontium ranelate treatment of human primary osteoblasts promotes an osteocyte-like phenotype while eliciting an osteoprotegerin response. Osteoporosis International **20(4),** 653-664.

Atsumi M, Park SH, Wang HL. 2007. Methods used to assess implant stability: current

status. International Journal of Oral and Maxillofacial Implants **22(5),** 743-754.

Azzawi ZG, Hamad TI, Kadhim SA, Naji GA. 2018. Osseointegration evaluation of laser-deposited titanium dioxide nanoparticles on commercially pure titanium dental implants, Journal of Materials Science: Materials in Medicine **29(7),** 96. http://dx.doi.org/10.1007/s10856-018-6097-6

Bhaskar SN, Orban BJ. 1991. Oral Histology And Embryology, 11E. Edition. St. Louis: Mosby. 178.

Bonnelye E, Chabadel A, Saltel F, Jurdic P. 2008. Dual effect of strontium ranelate: stimulation of osteoblast differentiation and inhibition of osteoclast formation and resorption in vitro, Bone, **42(1),** 129-138.

Buehler J, Chappuis P, Saffar JL, Tsouderos Y, Vignery A. 2001. Strontium ranelate inhibits bone resorption while maintaining bone formation in alveolar bone in monkeys (Macaca fascicularis), Bone, **29(2),** 176-179.

Canalis E, Hott M, Deloffre P, Tsouderos Y, Marie PJ. 1996. The divalent strontium salt S12911 enhances bone cell replication and bone formation in vitro, Bone **18(6),** 517-523.

Chang W, Tu C, Chen TH, Komuves L, Oda Y, Pratt SA, Miller S, Shoback D. 1999. Expression and signal transduction of calcium-sensing receptors in cartilage and bone, Endocrinology **140(12),** 5883-5893.

Capuccini C, Torricelli P, Sima F, Boanini E, Ristoscu C, Bracci B, Socol G, Fini M, Mihailescu IN, Bigi A. 2008. Strontium-substituted hydroxyapatite coatings synthesized by pulsed-laser deposition: in vitro osteoblast and osteoclast response, Acta biomaterialia **4(6),** 1885-1893.

Charyeva O, Altynbekov K, Zhartybaev R, Sabdanaliev A. 2012. Long-term dental implant success and survival--a clinical study after an observation period up to 6 years. Swedish dental journal **36(1),** 1-6.

Chattopadhyay N, Quinn SJ, Kifor O, Ye C, Brown EM. 2007. The calcium-sensing receptor (CaR) is involved in strontium ranelate-induced osteoblast proliferation. Biochemical Pharmacology, **74(3),** 438-447.

Cianferotti L, D'Asta F, Brandi ML. 2013. A review on strontium ranelate long-term antifracture efficacy in the treatment of postmenopausal osteoporosis. Therapeutic advances in musculoskeletal disease **5(3),** 127-139.

Dhert WJ, Klein CP, Jansen JA, Van der Velde EA, Vriesde RC, Rozing PM, De Groot K. 1993. A histological and histomorphometrical investigation of fluorapatite, magnesiumwhitlockite, and hydroxylapatite plasma-sprayed coatings in goats. Journal of Biomedical Materials Research **27(1),** 127-138.

Grynpas MD, Hamilton E, Cheung R, Tsouderos Y, Deloffre P, Hott M, Marie PJ. 1996. Strontium increases vertebral bone volume in rats at a low dose that does not induce detectable mineralization defect, Bone **18(3),** 253-259.

Hamad TI, Fatalla AA, Waheed AS, Azzawi ZG., Cao YG, Song K. 2018. Biomechanical Evaluation of Nano-Zirconia Coatings on Ti-6Al-7Nb Implant Screws in Rabbit Tibias. Current Medical Science **38(3),** 530-537.

Hassan AH, Al-Judy HJ, Fatalla AA. 2018. Biomechanical Effect of Nitrogen Plasma Treatment of Polyetheretherketone Dental Implant In Comparison To Commercially Pure Titanium. Journal of Research in Medical and Dental Science **6(2),** 367-377.

Hurtel-Lemaire AS, Mentaverri R, Caudrillier

A, Cournarie F, Wattel A, Kamel S, Terwilliger EF, Brown EM, Brazier M. 2009. The calcium-sensing receptor is involved in strontium ranelate-induced osteoclast apoptosis new insights into the associated signaling pathways, Journal of Biological Chemistry **284(1),** 575-584.

Jani GH, Al- Ameer SS. 2016. Mechanical Assessment of Oseointegration of Implant Coating with Mixture of Strontium Chloride and Hydroxyapatite at Different Concentration. International Journal of Science and Technology, **5(2),** 71-76.

Jung RE, Pjetursson BE, Glauser R, Zembic A, Zwahlen M, Lang NP. 2008. A systematic review of the 5-year survival and complication rates of implant-supported single crowns. Clinical oral implants research **19(2),** 119-130.

Kavitha M, Subramanian R, Vinoth KS, Narayanan R, Venkatesh G, Esakkiraja N. 2015. Optimization of process parameters for solution combustion synthesis of Strontium substituted Hydroxyapatite nanocrystals using Design of Experiments approach, Powder Technology **271,** 167-181.

Kim JR, Kim SH, Kim IR, Park BS, Kim YD. 2016. Low-level laser therapy affects osseointegration in titanium implants: resonance frequency, removal torque, and histomorphometric analysis in rabbits. Journal of the Korean Association of Oral and Maxillofacial Surgeons **42(1),** 2-8.

Li B, Liao X, Zheng L, Zhu X, Wang Z, Fan H, Zhang X. 2012. RETRACTED: Effect of nanostructure on osteoinduction of porous biphasic calcium phosphate ceramics, Acta Biomaterialia, **8(10),** 3794-3804.

Linder L. 1985. High-resolution microscopy of the implant-tissue interface, Acta Orthopaedica Scandinavica **56(3)**, 269-272.

Li Y, Li Q, Zhu S, Luo E, Li J, Feng G, Liao Y, Hu J. 2010. The effect of strontium-substituted hydroxyapatite coating on implant fixation in ovariectomized rats, Biomaterials **31(34),** 9006-9014.

Marie PJ, Hott M, Modrowski D, De-Pollak C, Guillemain J, Deloffre P, Tsouderos Y. 1993. An uncoupling agent containing strontium prevents bone loss by depressing bone resorption and maintaining bone formation in estrogen-deficient rats, Journal of Bone and Mineral Research **8(5),** 607-615.

Marquis RE. 1995. Antimicrobial actions of fluoride for oral bacteria. Canadian Journal of Microbiology, **41(11),** 955-964.

Marsh P, Martin M. 1999. Acquisition, adherence, distribution and metabolism of the oral microflora, p 34–57. Oral microbiology, 4th ed. Reed Educational and Professional Publishing Ltd., Bodmin, Cornwall, United Kingdom.

Mendonça G, Mendonça DB, Aragao FJ, Cooper LF. 2008. Advancing dental implant surface technology–from micron-to nanotopography. Biomaterials **29(28),** 3822-3835.

Ohno M, Kimoto K, Toyoda T, Kawata K, Arakawa H. 2013. Fluoride-treated bio-resorbable synthetic hydroxyapatite promotes proliferation and differentiation of human osteoblastic MG-63 cells, Journal of Oral Implantology **39(2),** 154-60.

O'Sullivan C, O'Hare P, O'Leary ND, Crean AM, Ryan K, Dobson AD, O'Neill L. 2010. Deposition of substituted apatites with anticolonizing properties onto titanium surfaces using a novel blasting process. Journal of Biomedical Materials Research Part B, Applied Biomaterials **95(1),** 141-149.

Park SH, Park KS, Cho SA. 2016. Comparison of removal torques of SLActive® implant and blasted,

laser-treated titanium implant in rabbit tibia bone healed with concentrated growth factor application. The Journal of Advanced Prosthodontics **8(2),** 110-115.

Qiao W, Liu R, Li Z, Luo X, Huang B, Liu Q, Chen Z, Tsoi JK, Su Y, Cheung K, Yeung KW. 2018. Targeted Release of Endogenous Cations from Xenograft Bone Driven by Fluoride Incorporation Contributes to Enhanced Bone Regeneration. Biomaterial Science **6(11),** 2951-2964.

Raucci MG, Giugliano D, Alvarez-Perez MA, Ambrosio L. 2015. Effects on growth and osteogenic differentiation of mesenchymal stem cells by the strontium-added sol–gel hydroxyapatite gel materials. Journal of Materials Science: Materials in Medicine **26(2),** 90. http://dx.doi.org/10.1007/s10856-015-5436-0.

Refaat MM, Hamad TI. 2016. Evaluation of mechanical and histological significance of nano hydroxyapatite and nano zirconium oxide coating on the osseointegration of CP Ti implants. Journal of Baghdad College of Dentistry **28(3),** 30-37.

Simonis P, Dufour T, Tenenbaum H. 2010. Long-term implant survival and success: a 10–16-year follow-up of non-submerged dental implants. Clinical Oral Implants research **21(7),** 772-777.

Takahashi N, Washio J. 2011. Metabolomic effects of xylitol and fluoride on plaque biofilm in vivo. Journal of Dental Research **90(12),** 1463-1468.

Vogel GL, Zhang Z, Chow LC, Schumacher GE. 2002. Changes in lactate and other ions in plaque and saliva after a fluoride rinse and subsequent sucrose administration, Caries research **36(1),** 44-52.

Whitford GM. 1999. Fluoride metabolism and excretion in children. Journal of Public Health Dentistry **59,** 224–228.

Xue W, Hosick HL, Bandyopadhyay A, Bose S, Ding C, Luk KD, Cheung KM, Lu WW. 2007. Preparation and cell–materials interactions of plasma sprayed strontium-containing hydroxyapatite coating. Surface and Coatings technology **201(8),** 4685-4693.

Zhang W, Wang G, Liu, Y, Zhao X, Zou D, Zhu C, Jin Y, Huang Q, Sun J, Liu X, Jiang X, Zreiqat H. 2013. The Synergistic Effect of Hierarchical Micro/Nano-Topography and Bioactive Ions for Enhanced Osseointegration, Biomaterials **34,** 3184-3195.